Two-dimensional Green's function theory for the electrodynamics of a rotating medium

Ben Zion Steinberg, Adi Shamir, and Amir Boag
School of Electrical Engineering, Tel Aviv University, Ramat-Aviv, Tel-Aviv 69978, Israel
(Received 29 March 2006; published 20 July 2006)

We derive an exact spectral representation for the Green's function of Maxwell equations in a two-dimensional homogeneous and rotating environment. The formulation is developed in the medium (noninertial) rest frame, and it represents the response to a point source, where both the source and observation points rotate together with the medium. The closed form expression for the Green's function is derived for (nonrelativistic) slowly rotating media at finite distances. An approximate expression for the efficient evaluation of the Green's function, that avoids laborious summation of rotating-medium spherical harmonics, is provided and tested against the exact expression. Furthermore, it is shown that our spectral theory can provide a broad view of the optical response of rotating systems, from which the classical Sagnac effect is obtained as a special case.

DOI: 10.1103/PhysRevE.74.016608 PACS number(s): 41.20.−q, 42.25.−p, 42.25.Bs, 42.70.Qs

I. INTRODUCTION

There is a recent interest in the theory and applications of rotating or accelerating optical systems that incorporate intricate scattering phenomena, such as photonic crystal (PhC) structures [1–3]. It was shown in Ref. [1] that a time-dependent analog of Floquet-Bloch theorem exists in a PhC that undergoes an accelerated motion, and that under certain conditions interesting interband transitions can take place. Translational and rotational symmetries of the electromagnetic modes of a rotating PhC structure have been reported [2]. These two works dealt with perfectly periodic PhCs and concentrated on the fundamental properties as seen in the laboratory (inertial) frame of reference. A more recent work [3] deals with the effect of rotation on a set of PhC microcavities, or local defects. The analysis is performed in the rotating PhC rest frame, which is noninertial. Specifically, it studies the dispersion properties of a slowly rotating set of weakly coupled microcavities, in which a novel manifestation of the Sagnac effect has been observed (see Ref. [4] for a review of the classical Sagnac effect). An application of this effect for the design of PhC-based optical gyroscopes has also been suggested [3]. Further application of this idea to a set of slowly rotating coupled microring resonators has been reported [5]. The works mentioned above have adopted diverse strategies to address the analytical challenges associated with the undertaking; direct modal analysis of time-dependent Maxwell's equation in the laboratory frame [1,2]; extension of tight-binding theory to electrodynamics of rotating medium [3]; or the extension of the transfer matrix method [5]. On a somewhat different track of study, numerical finite difference time domain (FDTD) methods were used to study time-dependent PhC structures [6,7].

In light of these new reports, we anticipate that the optics of slowly rotating or accelerating structures that support complex multiple scattering effects constitutes a new area of research of both theoretical and practical interest. Numerical algorithms can provide a vital tool for an accurate assessment of the analytical results, and for the design and optimization of optical devices based on the new theories. In developing such numerical tools, several basic considerations should be taken into account. First, when observed in the laboratory frame of reference, any rotating system inherently exhibits two widely differing time scales: one is defined by the optical frequency ω, and the other by the rotation frequency Ω. The large difference between these two scales introduces stiff requirements from the numerical code and needs special handling. Furthermore, it eliminates the pure time-harmonic nature of the system response. Formally, FDTD methods can provide the right answer for the latter difficulty. However, it is well known that FDTD may exhibit poor convergence and accuracy problems when dealing with high-Q electromagnetic systems such as the resonators in some of the above mentioned works [3,5].

An alternative approach is to perform the study in the system rest frame [3]. For slowly rotating systems, this yields a set of equations in which the rotation rate Ω appears as a small parameter within the medium constitutive relations [3,8], and *not* as a dynamic variable. This means that the time dependence $e^{-i\omega t}$ still constitutes a temporal eigensolution of Maxwell's equations in the system rest frame, so one can employ time-harmonic analysis. This is especially advantageous when high-Q resonators are under consideration, as in such cases time-harmonic approach is somewhat advantageous to FDTD based codes. Furthermore, in applications such as optical gyroscopes, the system response in its rest frame is the most relevant one, as it is directly connected to the actual measurements.

Numerical codes based on time-harmonic analysis, such as the classical method of moments (MOM) [9] or some of its relatives [10,11], require a prior knowledge of the Maxwell equations Green's function G of an appropriately defined background medium. When considering the rotation of optical systems, a convenient choice for G is the Green's function of a slowly rotating homogeneous medium, in the medium rest frame. This is the purpose of the present work. We start by a systematic development of the relevant wave equations that govern the fields in a slowly rotating two-dimensional homogeneous medium, in the medium rest frame. We show that the classical decomposition of the electromagnetic fields into independent TE and TM modes still holds, and we derive the wave equations for these two polarizations. Using the TE-TM decomposition, an exact scalarization of the vector wave equations is achieved. Then an exact spectral construction of the problem Green's function

is developed. This Green's function represents the response to a point source, where both the point source and the observer rotate together with the medium. Our spectral construction provides an exact representation of the new Green's function via a summation of cylindrical Harmonics. An approximate expression, using an expansion based on the small parameter Ω/ω, is provided too. This approximation does not need a summation of the cylindrical Harmonics series, and is expressed via the well-known stationary medium Green's function. We study the effect of rotation on the new solution and its approximation, and compare it to the Green's function of a stationary medium.

To demonstrate the efficacy of our spectral theory for a detailed study of rotating optical systems, and its ability to provide a somewhat broader view of the physics involved, we use the new Green's function in order to obtain the effect of rotation on a circular resonator. We obtain the effect of rotation on the entire set of resonances that constitute the system response, and show that the classical Sagnac effect can be obtained from this general spectral study as a special case that pertains to a limited portion of the system spectrum.

Finally, we note that the theory developed here applies to two-dimensional configurations. However, there are many practical three-dimensional geometries of interest, for which propagation and scattering analysis based on two-dimensional theories can be used. For example, two-dimensional (2D) realizations of PhC structures and high-Q microcavities in dielectric slabs were studied by several research groups [12,13], and offer practical realization of PhC structures and microcavities. Here, the guiding or confinement of the fields in directions parallel to the slab plane are provided by a two-dimensional periodic structure, while the total internal reflection phenomenon prevents scattering off the slab plane, thus providing a confinement in the direction normal to the slab. It has been shown that for the frequency range that corresponds to the lowest guided mode in the slab, the properties of such structures can be approximated by an ideal 2D structure using the effective index approach [12]. In principle, a similar strategy can be used in order to apply our rotating-medium Green's function to study realistic 3D rotating PhCs. The extension of the theory developed in this paper to handle a full three-dimensional Green's function construction is currently under study.

The structure of the paper is as follows. In Sec. II we develop the basic wave equation and introduce the TE-TM decomposition. Section III deals with the exact spectral construction of the rotating medium Green's function via cylindrical Harmonics series, and its approximate expression. Spectral analysis of a simple example of ring resonator, and the interpretation of Sagnac effect as a special case, are discussed in Sec. IV. Physical interpretations of the mathematical results obtained here, and some important observations pertaining to actual computational implementations, are provided in Sec. V. Concluding remarks are provided in Sec. VI.

II. GENERAL EQUATIONS

Let a homogeneous medium rotate at an angular velocity $\mathbf{\Omega}$ around the center of a coordinate system $\boldsymbol{r}=0$. The medium is at rest in the noninertial reference frame $\mathcal{R}:(x',y',z')$. Without loss of generality, we assume that the rotation is around the z axis, so we have

$$\mathbf{\Omega} = \hat{z}\Omega, \tag{2.1a}$$

where Ω is a scalar measuring the angular velocity magnitude; it possesses positive or negative sign for counterclockwise or clockwise rotations, respectively. Thus

$$\begin{pmatrix} x' \\ y' \\ z' \end{pmatrix} = \begin{pmatrix} \cos(\Omega t) & \sin(\Omega t) & 0 \\ -\sin(\Omega t) & \cos(\Omega t) & 0 \\ 0 & 0 & 1 \end{pmatrix} \begin{pmatrix} x \\ y \\ z \end{pmatrix}. \tag{2.1b}$$

Our purpose now is to solve Maxwell's equations in the rotating system $\mathcal{R}$. A few important points are observed: (i) In $\mathcal{R}$, the system properties do not vary in time. (ii) The angular velocity Ω and the medium maximal dimension L satisfy $|\Omega L| \ll c$. Therefore no relativistic effects take place. (iii) Consistent with the slow velocity assumption above, no geometrical transformations or deformations take place. Thus, for example, the ∇ operator is conserved: $\nabla = \nabla'$. For the very same reason, time is invariant in both systems: $t = t'$.

According to the formal structure of electrodynamics, the basic physical laws are invariant under *all* space-time transformations (including noninertial ones). Therefore the charge-free Maxwell's equations in $\mathcal{R}$ are given by [8]

$$\nabla' \times \boldsymbol{E}' = i\omega \boldsymbol{B}' - \boldsymbol{J}^{\mathrm{M}'}, \quad \nabla' \cdot \boldsymbol{B}' = 0, \tag{2.2a}$$

$$\nabla' \times \boldsymbol{H}' = -i\omega \boldsymbol{D}' + \boldsymbol{J}', \quad \nabla' \cdot \boldsymbol{D}' = 0, \tag{2.2b}$$

where we have added a fictitious magnetic current density $\boldsymbol{J}^{\mathrm{M}'}$. A time harmonic dependence $e^{-i\omega t}$ is assumed and suppressed throughout. The transformation from the inertial system $\mathcal{I}$ to the rotating one $\mathcal{R}$ is manifested via the local constitutive relations. Let the material properties at rest be given by ϵ, μ. Then up to the first order in velocity the constitutive relations in $\mathcal{R}$ take on the form [8]

$$\boldsymbol{D}' = \epsilon \boldsymbol{E}' - c^{-2}\mathbf{\Omega} \times \boldsymbol{r}' \times \boldsymbol{H}', \tag{2.3a}$$

$$\boldsymbol{B}' = \mu \boldsymbol{H}' + c^{-2}\mathbf{\Omega} \times \boldsymbol{r}' \times \boldsymbol{E}', \tag{2.3b}$$

where c is the "stationary vacuum" speed of light: the vacuum light velocity as observed in the stationary system. All subsequent derivations are performed in the rotating reference frame $\mathcal{R}:(x',y',z')$, and all physical and geometrical quantities refer to those measured in this frame. Thus for simplicity we omit the prime. We rewrite the ∇ operator as a summation of two operators $\nabla = \nabla_t + \hat{z}\partial_z$, where $\nabla_t \equiv \hat{\boldsymbol{x}}\partial_x + \hat{\boldsymbol{y}}\partial_y$ refers to derivatives in the transverse (to $\hat{z}$) directions only. Likewise, any vector quantity can be separated into transverse and $\hat{z}$ polarized quantities: $\boldsymbol{E} = \boldsymbol{E}_t + \hat{z}E_z$. Since the rotation axis coincides with $\hat{z}$, it is convenient to use a cylindrical coordinate system $\boldsymbol{r} = (\rho, \theta, z)$ in which for any vector field $\boldsymbol{V}$ we have [see Eq. (2.1a)]

$$\boldsymbol{\Omega}\times\boldsymbol{r}\times\boldsymbol{V}=\boldsymbol{\rho}\Omega V_z-\hat{z}\Omega\rho V_\rho, \tag{2.4}$$

where we use the notation $\boldsymbol{\rho}\equiv\hat{\boldsymbol{\rho}}\rho$. Maxwell equations can now be written as

$$\nabla_t\times\boldsymbol{E}_t+\hat{z}\partial_z\times\boldsymbol{E}_t+\nabla_t\times\hat{z}E_z = \hat{z}i\omega(\mu H_z-\Omega c^{-2}\rho E_\rho)+i\omega(\mu\boldsymbol{H}_t+\Omega c^{-2}\boldsymbol{\rho}E_z)-\boldsymbol{J}^M \tag{2.5a}$$

$$\nabla_t\times\boldsymbol{H}_t+\hat{z}\partial_z\times\boldsymbol{H}_t+\nabla_t\times\hat{z}H_z = -\hat{z}i\omega(\epsilon E_z+\Omega c^{-2}\rho H_\rho)-i\omega(\epsilon\boldsymbol{E}_t-\Omega c^{-2}\boldsymbol{\rho}H_z)+\boldsymbol{J}. \tag{2.5b}$$

The first term on the left-hand side and the first two terms on the right-hand side of the equations above are $\hat{z}$ directed, and the rest field terms are transversely directed.

A. TM and TE modes in homogeneous medium

Assume that $\partial_z\equiv 0$. The last equations read

$$\nabla_t\times\boldsymbol{E}_t+\nabla_t\times\hat{z}E_z=\hat{z}i\omega(\mu H_z-\Omega c^{-2}\rho E_\rho)+i\omega(\mu\boldsymbol{H}_t+\Omega c^{-2}\boldsymbol{\rho}E_z)-\boldsymbol{J}^M, \tag{2.6a}$$

$$\nabla_t\times\boldsymbol{H}_t+\nabla_t\times\hat{z}H_z=-\hat{z}i\omega(\epsilon E_z+\Omega c^{-2}\rho H_\rho)-i\omega(\epsilon\boldsymbol{E}_t-\Omega c^{-2}\boldsymbol{\rho}H_z)+\boldsymbol{J}. \tag{2.6b}$$

It is seen now that Eqs. (2.6a) and (2.6b) can be satisfied using two independent sets of fields:

(i) *TM fields* (*or E polarization*). In this set we have $\boldsymbol{E}_t=\boldsymbol{0}$, $H_z=0$, $J_z^{\mathrm{M}}=0$, while in general the field quantities E_z, $\boldsymbol{H}_t$ and currents J_z, $\boldsymbol{J}_t^M$ are not necessarily zero. This case can be completely characterized by the scalar E_z.

(ii) *TE fields* (*or H polarization*). Here $\boldsymbol{H}_t=\boldsymbol{0}$, $E_z=0$, $J_z=0$, while in general the field quantities H_z, $\boldsymbol{E}_t$ and currents J_z^{M}, $\boldsymbol{J}_t$ are not necessarily zero. This case can be completely characterized by the scalar H_z.

Below we derive specific wave equations for each polarization.

1. TM wave equation

For the TM case, Eqs. (2.6a) and (2.6b) reduce to

$$\nabla_t\times\hat{z}E_z=i\omega(\mu\boldsymbol{H}_t+\Omega c^{-2}\boldsymbol{\rho}E_z)-\boldsymbol{J}_t^M, \tag{2.7a}$$

$$\nabla_t\times\boldsymbol{H}_t=-\hat{z}i\omega(\epsilon E_z+\Omega c^{-2}\rho H_\rho)+\hat{z}J_z. \tag{2.7b}$$

From Eq. (2.7a), we can express $\boldsymbol{H}_t$ in terms of the scalar field E_z and the currents

$$i\omega\mu\boldsymbol{H}_t=\boldsymbol{J}_t^M+\nabla_t\times\hat{z}E_z-i\omega\Omega c^{-2}\boldsymbol{\rho}E_z. \tag{2.8}$$

We substitute this expression back into Eq. (2.7b) and use the identities $\nabla_t\times\nabla_t\times\hat{z}E_z=-\hat{z}\nabla_t^2E_z$ and $H_\rho=\hat{\boldsymbol{\rho}}\cdot\boldsymbol{H}_t$. Up to first order terms in Ω, the result is

$$-\hat{z}(\nabla_t^2+k_0^2n^2)E_z-i\omega\Omega c^{-2}\nabla_t\times(\boldsymbol{\rho}E_z)+i\omega\Omega c^{-2}\times[\boldsymbol{\rho}\cdot(\nabla_t\times\hat{z}E_z)]\hat{z} = \hat{z}i\omega\mu J_z-\hat{z}i\omega\Omega c^{-2}\boldsymbol{\rho}\cdot\boldsymbol{J}_t^M-\nabla_t\times\boldsymbol{J}_t^M, \tag{2.9}$$

where $k_0=\omega/c$ is the vacuum wave number, and $n=\sqrt{\mu_r\epsilon_r}$ is the medium refraction index, as measured for a stationay medium ($\Omega=0$). By a straight forward application of the vector operations, it can be shown that

$$\hat{z}\cdot\nabla_t\times(\boldsymbol{\rho}E_z)=-[\boldsymbol{\rho}\cdot(\nabla_t\times\hat{z}E_z)]=(y\partial_x-x\partial_y)E_z=-\partial_\theta E_z, \tag{2.10}$$

thus Eq. (2.9) is reduced to

$$[\nabla_t^2+k_0^2n^2]E_z-2ik_0^2\frac{\Omega}{\omega}\partial_\theta E_z=S^{\mathrm{TM}}, \tag{2.11a}$$

where S^{TM} is the TM scalar source term given by

$$S^{\mathrm{TM}}=-i\omega\mu J_z+i\omega\Omega c^{-2}\boldsymbol{\rho}\cdot\boldsymbol{J}_t^M+\hat{z}\cdot\nabla_t\times\boldsymbol{J}_t^M. \tag{2.11b}$$

2. TE wave equation

For the TE case, Eqs. (2.6a) and (2.6b) reduce to

$$\nabla_t\times\boldsymbol{E}_t=\hat{z}i\omega(\mu H_z-\Omega c^{-2}\rho E_\rho)-\hat{z}J_z^{\mathrm{M}}, \tag{2.12a}$$

$$\nabla_t\times\hat{z}H_z=-i\omega(\epsilon\boldsymbol{E}_t-\Omega c^{-2}\boldsymbol{\rho}H_z)+\boldsymbol{J}_t. \tag{2.12b}$$

From Eq. (2.12b), we can express $\boldsymbol{E}_t$ in terms of the scalar field H_z and the currents

$$i\omega\epsilon\boldsymbol{E}_t=\boldsymbol{J}_t-\nabla_t\times\hat{z}H_z+i\omega\Omega c^{-2}\boldsymbol{\rho}H_z. \tag{2.13}$$

The derivation now is completely symmetrical to the TM case. The result is

$$[\nabla_t^2+k_0^2n^2]H_z-2ik_0^2\frac{\Omega}{\omega}\partial_\theta H_z=S^{\mathrm{TE}}, \tag{2.14a}$$

where S^{TE} is the TE scalar source term given by

$$S^{\mathrm{TE}}=-i\omega\epsilon J_z^{\mathrm{M}}-i\omega\Omega c^{-2}\boldsymbol{\rho}\cdot\boldsymbol{J}_t-\hat{z}\cdot\nabla_t\times\boldsymbol{J}_t. \tag{2.14b}$$

III. GREEN'S FUNCTION G AND ITS SPECTRAL CONSTRUCTION

We are interested in deriving the Green's function for the wave operator in Eq. (2.11a) or Eq. (2.14a). This Green's function $G^{\mathrm{TM,TE}}$ satisfies the same wave equation with the source term $S^{\mathrm{TM,TE}}$ replaced by a two-dimensional unit point source located at $\boldsymbol{\rho}'=(x',y')$ [or (ρ',θ') in cylindrical coordinate]. Such sources can be expressed as

$$\boldsymbol{J}=\hat{z}I_z\delta(x-x')\delta(y-y') \quad \text{and} \quad \boldsymbol{J}^M=0, \quad \text{for TM}, \tag{3.1a}$$

$$\boldsymbol{J}^M=\hat{z}I_z^{\mathrm{M}}\delta(x-x')\delta(y-y') \quad \text{and} \quad \boldsymbol{J}=0, \quad \text{for TE}, \tag{3.1b}$$

where I_z, I_z^{M} are unit currents. Thus we seek a solution of the canonical problem

$$\frac{1}{\rho}\partial_\rho[\rho\partial_\rho G] + \frac{1}{\rho^2}\partial_\theta^2 G + k_0^2 n^2 G - 2ik_0^2\frac{\Omega}{\omega}\partial_\theta G = -\frac{1}{\rho'}\delta(\rho-\rho')\delta(\theta-\theta'), \tag{3.2}$$

where for the TM or TE wave excitation, we have

$$G^{\mathrm{TM}} = i\omega\mu I_z G, \quad G^{\mathrm{TE}} = i\omega\epsilon I_z^{\mathrm{M}} G. \tag{3.3}$$

Note that the medium is homogeneous in θ (i.e., the coefficients of this equation are θ independent). We therefore suggest the following transformation pair:

$$G(\rho,\theta;\rho',\theta') = \frac{1}{2\pi}\sum_{m=-\infty}^{\infty}\tilde{g}_m(\rho,\rho';\theta')e^{im\theta}, \tag{3.4}$$

$$\tilde{g}_m(\rho,\rho';\theta') = \int_0^{2\pi} G(\rho,\theta;\rho',\theta')e^{-im\theta}d\theta. \tag{3.5}$$

Applying this to Eq. (3.2), we get an ordinary differential equation for $\tilde{g}_m$:

$$\frac{1}{\rho}\frac{d}{d\rho}\left[\rho\frac{d}{d\rho}\tilde{g}_m\right] - \frac{m^2}{\rho^2}\tilde{g}_m + k_0^2 n^2\gamma_m^2\tilde{g}_m = -\frac{1}{\rho'}\delta(\rho-\rho')e^{-im\theta'}, \tag{3.6}$$

where we have defined

$$\gamma_m^2 = 1 + 2m\frac{\Omega}{\omega n^2}. \tag{3.7}$$

The structure of Eq. (3.6) means that we can express $\tilde{g}_m(\rho,\rho';\theta')$ as a multiplication of a 1D Green's function in ρ, with $e^{-im\theta'}$,

$$\tilde{g}_m(\rho,\rho';\theta') = \tilde{g}_{\rho,m}(\rho,\rho')e^{-im\theta'}, \tag{3.8}$$

where $\tilde{g}_{\rho,m}(\rho,\rho')$ satisfies

$$\frac{1}{\rho}\frac{d}{d\rho}\left[\rho\frac{d}{d\rho}\tilde{g}_{\rho,m}\right] - \frac{m^2}{\rho^2}\tilde{g}_{\rho,m} + k_0^2 n^2\gamma_m^2\tilde{g}_{\rho,m} = -\frac{1}{\rho'}\delta(\rho-\rho'). \tag{3.9}$$

This equation possesses a structure amenable to an exact solution procedure based on the standard resolvent theory—see, for example, Chap. 3.4c in Ref. [16]. It is given by

$$\tilde{g}_{\rho,m}(\rho,\rho') = \frac{\pi i}{2}J_m(k_0 n\gamma_m\rho_<)H_m^{(1)}(k_0 n\gamma_m\rho_>), \tag{3.10a}$$

where

$$\rho_< \equiv \min(\rho,\rho'), \quad \rho_> \equiv \max(\rho,\rho') \tag{3.10b}$$

and where the branch cut for γ_m in the γ_m^2 plane [see Eq. (3.7)] extends from the branch point at the origin, running along and just below the negative real axes to $-\infty$. This choice of cut ensures that

$$\mathrm{Re}\ \gamma_m \geq 0, \quad \mathrm{Im}\ \gamma_m \geq 0. \tag{3.10c}$$

The first requirement above is needed to ensure smooth analytic continuation of the $\Omega=0$ case. The second requirement stems from the properties of the Hankel and Bessel functions of complex argument, and is formally needed in order to ensure convergence at infinity of the (extremely) high order negative (for $\Omega>0$) or positive (for $\Omega<0$) harmonics, for which $m\Omega<-\omega n^2/2$. Note that in practice this formal requirement is hardly needed.

Collecting Eqs. (3.4) and (3.8) together and using Eq. (3.10a), we get a simple expression for the full 2D Green's function,

$$G(\rho,\theta;\rho',\theta') = \frac{1}{2\pi}\sum_{m=-\infty}^{\infty}\tilde{g}_{\rho,m}(\rho,\rho')e^{im(\theta-\theta')} \tag{3.11}$$

or

$$G = \frac{i}{4}\sum_{m=-\infty}^{\infty}J_m(k_0 n\gamma_m\rho_<)H_m^{(1)}(k_0 n\gamma_m\rho_>)e^{im(\theta-\theta')}. \tag{3.12}$$

This equation constitutes a spectral representation of the Green's function of rotating medium, in its rest frame. It is exact under the assumption of slow rotation, detailed in item (ii) in the beginning of Sec. II. Note that the information regarding the medium rotation is manifested only via the role of γ_m. Note its dependence on the small parameter Ω/ω. Depending on the magnitude and direction of rotation, γ_m increases or decreases the effective wavelength. The effect of rotation is demonstrated graphically in Sec. III B.

A. Efficient computation for small Ω/ω

Let the Green function of a stationary (nonrotating) medium be denoted by G^{st}. It is obtained from the formulation of the previous subsections by setting $\gamma_m=1\ \forall m$, and can be expressed as

$$G^{\mathrm{st}} = \frac{i}{4}\sum_{m=-\infty}^{\infty}J_m(k_0 n\rho_<)H_m^{(1)}(k_0 n\rho_>)e^{im(\theta-\theta')} = \frac{i}{4}H_0^{(1)}(k_0 n|\boldsymbol{\rho}-\boldsymbol{\rho}'|). \tag{3.13}$$

For slow rotation rates, we can approximate

$$\gamma_m \approx 1 + m\frac{\Omega}{n^2\omega} \Rightarrow k_0 n\gamma_m\rho \approx k_0 n\rho + m\frac{\Omega}{n\omega}k_0\rho \tag{3.14a}$$

provided that the harmonics index m does not get too large. That is,

$$\frac{|m\Omega|}{\omega} \ll n^2. \tag{3.14b}$$

It should be emphasized that in practice Ω is smaller than ω by many orders of magnitude, while for sufficient accuracy the range of summation over m is of the order of a few

hundreds, at most. Therefore it is not difficult to satisfy condition (3.14b). Then, we can expand the Bessel and Hankel functions around $\Omega/\omega=0$ to first order in $(\Omega/\omega)k_0\rho$,

$$J_m(k_0 n\gamma_m\rho_<) \approx J_m(k_0 n\rho_<) + m\frac{\Omega}{n\omega}k_0\rho_< J_m'(k_0 n\rho_<), \tag{3.15a}$$

$$H_m^{(1)}(k_0 n\gamma_m\rho_>) \approx H_m^{(1)}(k_0 n\rho_>) + m\frac{\Omega}{n\omega}k_0\rho_> H_m^{(1)'}(k_0 n\rho_>). \tag{3.15b}$$

Here the prime denotes a derivative with respect to the argument. This approximation puts an additional constraint:

$$\frac{|m\Omega|}{\omega}k_0\max(\rho,\rho') \ll n. \tag{3.15c}$$

Considering the condition in Eq. (3.14b) and the discussion thereafter, the last inequality actually states that ρ and ρ' can be of the order of few wavelengths or even tens of wavelengths. Substituting this result back into the expansion for G in Eq. (3.12), using Eq. (3.13), and keeping terms up to the first order in Ω/ω, we obtain

$$G = G^{\mathrm{st}} + \frac{i}{4}\sum_m \frac{m\Omega}{n\omega}k_0\rho_< J_m'(k_0 n\rho_<)H_m^{(1)}(k_0 n\rho_>)e^{im(\theta-\theta')} + \frac{i}{4}\sum_m \frac{m\Omega}{n\omega}k_0\rho_> J_m(k_0 n\rho_<)H_m^{(1)'}(k_0 n\rho_>)e^{im(\theta-\theta')}. \tag{3.16}$$

Owing to the structure of the expressions above, we can replace m by $-i\partial_\theta$ and replace $k_0 J_m'(k_0 n\rho_<)$ by $n^{-1}\partial_{\rho_<} J_m(k_0 n\rho_<)$. Using these identities and Eq. (3.13), we finally obtain an approximate expression,

$$G_{\mathrm{app}} = G^{\mathrm{st}} - i\frac{\Omega}{n^2\omega}\partial_\theta(\rho\partial_\rho + \rho'\partial_{\rho'})G^{\mathrm{st}}, \tag{3.17}$$

that can be readily evaluated from the stationary medium Green's function G^{st}, with no series summation. The result is

$$G_{\mathrm{app}} = G^{\mathrm{st}}\left[1 + i\frac{\Omega}{\omega}k_0^2\rho\rho'\sin(\theta-\theta')\right] + \mathcal{O}\{(\Omega/\omega)^2\} = G^{\mathrm{st}}\left[1 + i\frac{\Omega}{\omega}k_0^2(yx'-xy')\right] + \mathcal{O}\{(\Omega/\omega)^2\}, \tag{3.18}$$

where $k_0=\omega/c$, with c being the stationary vacuum speed of light. Continuing along these lines, the term in the square brackets can be viewed as a Taylor series expansion of an exponential. Thus it leads to

$$G_{\mathrm{app}} \approx G^{\mathrm{st}}e^{i(\Omega/\omega)k_0^2\rho\rho'\sin(\theta-\theta')} = G^{\mathrm{st}}e^{i(\Omega/\omega)k_0^2(yx'-xy')} = G^{\mathrm{st}}e^{i(\Omega/\omega)k_0^2\,\hat{z}\cdot(\boldsymbol{\rho}'\times\boldsymbol{\rho})}. \tag{3.19}$$

These expressions are tested in Sec. III B against the spectral summation of Eq. (3.12) which is exact under the slow rotation approximation.

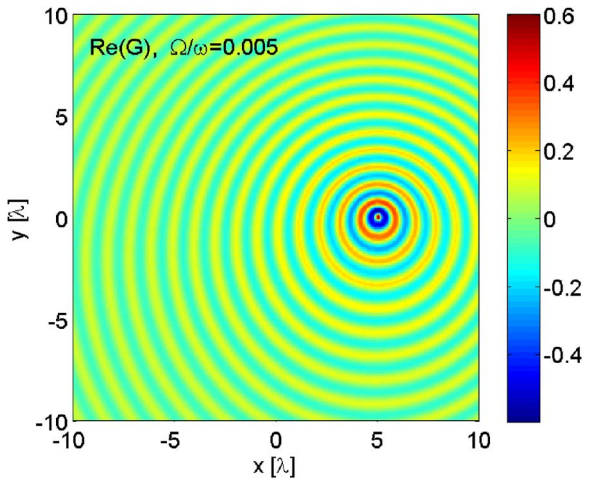

FIG. 1. (Color online) Real part of the rotating system Green's function in the x,y plane, for $(x',y')=(5,0)\lambda$.

B. Computation of G

We turn now to compute G exactly via the summation in Eq. (3.12) in order to demonstrate the effect of rotation, and to compare this exact calculation to the approximate one in Eqs. (3.18) and (3.19). Figure 1 shows an example of G in the x,y plane for $(x',y')=(5,0)\lambda$, where λ is the wavelength in the corresponding stationary problem. In order to notice the effect on the plot, the rotation speed Ω has been exaggerated; the computation is performed for $\Omega/\omega=5\times10^{-3}$. The exact summation formula in Eq. (3.12) has been used, with the summation range $|m|\le 80$. The axes dimensions are normalized to λ. Due to rotation, the radiation wavelength for $y>0$ $(y<0)$ in the source vicinity is slightly smaller (larger) than that of the stationary system wavelength. Note that the entire system (source, medium, and observer) rotates in a counterclockwise direction around the origin of this plot. Therefore the variations of wavelength can be interpreted as a local Doppler-like shifts, as seen in the rotating system rest frame. This is consistent with the observation made in Sec. V A.

Figure 2 shows the radial dependence of G for sources at the same location $[(x',y')=(5,0)\lambda]$—along the line $\theta=\pi/10$ radian. Rotation rate here is $\Omega/\omega=10^{-3}$. The summation range for the exact G here is $|m|\le 200$. The effect of rotation along this line is clearly seen; the wavelength is slightly increased (decreased) for $\rho<\rho'$ $(\rho>\rho')$. The lines designated by approximation 1 and approximation 2 show the approximate expressions in Eqs. (3.18) and (3.19), respectively. For the rotation speed and radial line shown both approximate expressions reconstruct the features of G quite well, but the accuracy of Eq. (3.19) is superior: within the graphical resolution it is indistinguishable from the exact spectral expansion.

Figure 3 shows the same G as of the previous figure, but as observed along an azimuthal track $\rho=5.1\lambda$. Again, the effect of rotation slightly decreases (increases) the wavelength for $\theta<\pi$ $(\theta>\pi)$. For the rotation speeds shown, the approximate expression of Eq. (3.18) reconstructs the field phase quite accurately, but field amplitude decreases in accu-

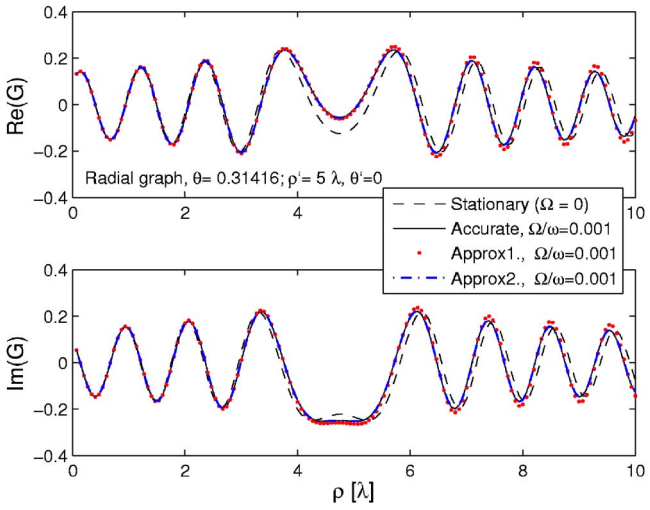

FIG. 2. (Color online) The Green's function versus radius for $\theta=\pi/10$ and for source point at the same location as in Fig. 1 $(\rho',\theta')=(5\lambda,0)$.

racy as θ approaches $\pi/2$ and $3\pi/2$. It is seen again that the approximation of Eq. (3.19) is superior, and it cannot be distinguished from the exact G within the graphical resolution of the figure.

The global features of G and its approximation are demonstrated in Figs. 4 and 5. In both figures, the source is located at $(x',y')=(5,0)\lambda$, the normalized rotation rate is $\Omega/\omega=10^{-4}$, and the summation range for the exact G is $|m|\leq 300$. A logarithmic scale is used in order to increase the dynamic range. Figure 4 compares the rotating medium Green's function to that of the stationary one, in the (x,y) plane. It is seen that in a direction perpendicular to the source movement vector, the field is practically identical to the field of a stationary system. The effect of rotation is maximal along the lines that are tangent to the source velocity vector. Recalling the results shown in Figs. 2 and 3, we conclude that this effect is essentially due to phase differences. Finally, Fig. 4 shows the error associated with approximation 2 of G

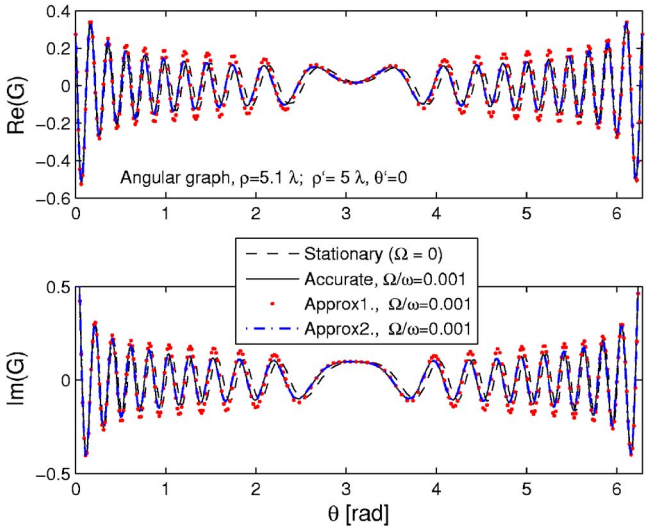

FIG. 3. (Color online) G along an angular line.

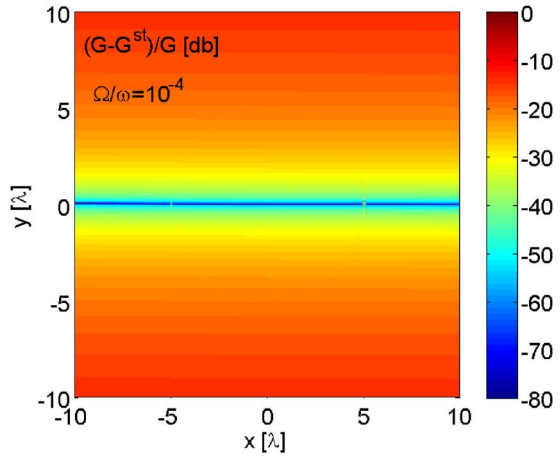

FIG. 4. (Color online) Normalized difference between the stationary and rotating medium Green's function, $|(G-G^{st})/G|$ in dB, showing the effect of rotation in the (x,y) plane.

discussed in Sec. III A [see Eq. (3.19)]. Note that in order to expand correctly the field around $\rho=\rho'$ and especially the singularity at $\boldsymbol{r}=\boldsymbol{r}'$, a very large number of harmonics is needed. Furthermore, it is well known that the Green's function structure near the source (at $\boldsymbol{r}=\boldsymbol{r}'$) depends solely on the differential equation order and dimensions (number of independent variables), while it is independent of the equation coefficients. Thus, at this neighborhood, the expression for G_{app} in Eq. (3.19), that is based on the analytically known stationary medium G and does not require a summation over cylindrical harmonics, is considered to be more accurate.

IV. EXAMPLE: ROTATING RING RESONATOR AND SAGNAC EFFECT

In this section we demonstrate the efficacy of our previous results in determining some of the fundamental electro-

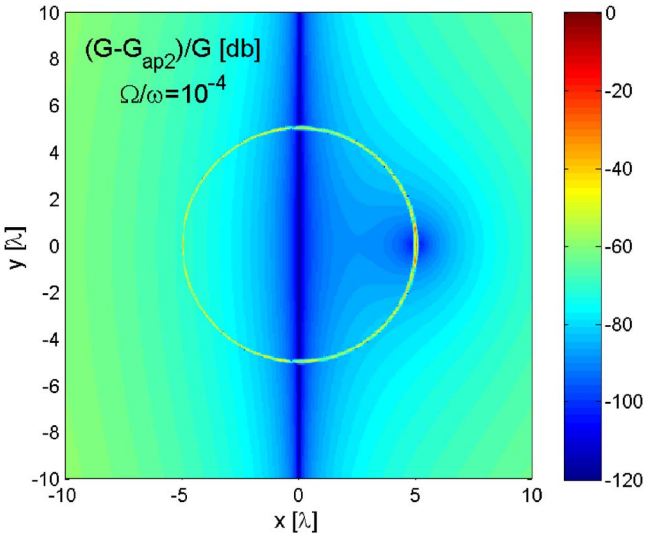

FIG. 5. (Color online) Normalized error of Green's function evaluation, $|(G-G_{app})/G|$ in dB, showing the quality of the approximation discussed in Sec. III A.

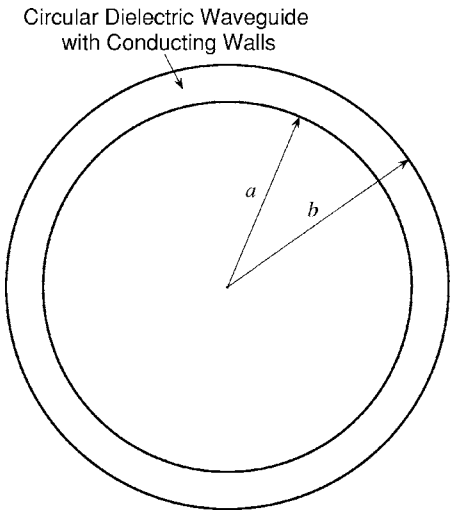

FIG. 6. The circular resonator.

magnetic properties of a rotating system; namely, its resonant frequencies and their relation to those of the stationary (nonrotating) system. To allow for analytic derivations that will make the physical interpretations as transparent as possible, we consider a relatively simple geometry shown in Fig. 6. A ring with the inner and outer radii denoted a and b, respectively, is filled with a dielectric material. The ring surfaces are perfect electric conductors. A scalar integral equation formulation that governs the TM eigenmodes (i.e., the source-free solution) supported by the structure is given by

$$\int_{\sigma} G(\rho,\theta;\rho',\theta')J_z(\rho',\theta')ds' = 0 \quad \forall\ (\rho,\theta) \in \sigma, \tag{4.1a}$$

where σ denotes the electrically conducting surfaces of the ring, and J_z is the z-directed electric current on the ring surfaces. Due to the $e^{im\theta}$ dependence of the Green's function mth harmonic, we anticipate the following form for the eigenmodes current $J_z^{(m')}$:

$$J_z^{(m')} = e^{im'\theta}\left[\frac{c_1}{a}\delta(\rho-a) + \frac{c_2}{b}\delta(\rho-b)\right],$$

$$m' = 0, \pm 1, \pm 2, \ldots, \tag{4.1b}$$

where c_1, c_2 are the inner and outer current excitation amplitudes, respectively. Note that the same scalar formulation governs the TE modes of a structure with perfect magnetic conductor walls and z-directed magnetic current. We substitute now the Green's function expansion of Eq. (3.12) into Eq. (4.1a) and perform the integration, utilizing the orthogonality of the exponential function. The result is the following matrix equation for the current excitation amplitudes c_1, c_2

$$\begin{pmatrix} H_m^{(1)}(k_0 n\gamma_m a) & H_m^{(1)}(k_0 n\gamma_m b) \\ J_m(k_0 n\gamma_m a) & J_m(k_0 n\gamma_m b) \end{pmatrix} \begin{pmatrix} c_1 \\ c_2 \end{pmatrix} = \begin{pmatrix} 0 \\ 0 \end{pmatrix}. \tag{4.2}$$

A nontrivial solution is allowed by equating the determinant to zero,

$$H_m^{(1)}(k_0 n\gamma_m a)J_m(k_0 n\gamma_m b) - H_m^{(1)}(k_0 n\gamma_m b)J_m(k_0 n\gamma_m a) = 0. \tag{4.3}$$

The roots of this equation $k_0 = k_0(\Omega,m) = \omega(\Omega,m)/c$ constitute the mth resonance of the system and determine its dependence on the rotation rate Ω. Note, however, that for the stationary system $\gamma_m = 1$. Since γ_m is the only parameter that depends on Ω, and it appears as a multiplicative factor in each of the $H_m^{(1)}, J_m$ arguments, we can relate the rotating system resonant frequency $\omega(\Omega,m)$ to that of the stationary system $\omega(0,m)$ via

$$\omega(\Omega,m)\gamma_m = \omega(0,m), \quad \gamma_m^2 = 1 + 2m\Omega/(\omega(\Omega,m)n^2). \tag{4.4}$$

Solving for $\omega(\Omega,m)$ and keeping terms up to the first order in Ω, we obtain

$$\omega(\Omega,m) = \omega(0,m) - m\Omega/n^2 + \mathcal{O}\{[m\Omega/n^2]^2/\omega(0,m)\}. \tag{4.5}$$

Thus rotation causes a shift of the resonance frequencies. For spatial harmonics that propagate in a direction that coincides with rotation, $m\Omega$ is positive and thus the resonant frequency decreases. For spatial harmonics that propagate in a direction counter to rotation, $m\Omega$ is negative, thus increasing the corresponding resonance frequency. It is interesting to note that from Eq. (4.5), the spectral *shifts* do not depend on the loop geometry (namely radius and width). This result is seemingly contradictive to the well known and classical Sagnac effect [4]. We unfold this apparent inconsistency in the next subsection.

Sagnac effect

The phase accumulated by a light beam that propagates along a slowly rotating circular path, depends linearly on the path angular velocity Ω, and on the area enclosed by the path. This phenomenon is known as the Sagnac effect [4]. When the circular path forms a complete loop resonator, the aforementioned phase shift causes an Ω dependent shift in the resonance frequencies. The difference between the co-rotation resonance and counter-rotation resonance is used in optical gyroscopes to determine the system rotation rate [15].

The Green's function theory and the ensuing analysis of the complete spectral properties of a closed ring structure, reported in the present work, constitute a formal mathematical tool from which the classical Sagnac effect can be derived as a special case. This special case pertains to a limited portion of the system spectrum. To demonstrate this, let us examine the spectral shifts effect shown in Eq. (4.5) on the spatial harmonics for which $m = \pm 2\pi Rn/\lambda$, where $R = (a+b)/2$ is the average ring radius, and λ is the corresponding

stationary vacuum wavelength. For a ring with $a \gg \lambda$ and $b-a \ll a$, these harmonics represent azimuthal propagation; they constitute propagation modes whose spatial wave number is locally tangent to the ring center line $\rho=R$. For these modes we have the resonant frequencies $\omega^{\pm}$,

$$\omega^{\pm} = \omega(0,m) \mp \frac{2\pi R}{\lambda n}\Omega, \tag{4.6}$$

which is exactly the classical co-rotation and counter-rotation resonances resulting from the classical Sagnac effect [4].

V. PHYSICAL INTERPRETATIONS AND NUMERICAL IMPLEMENTATION

A. Physical interpretation

In Sec. III B, we have shown that the simple expression in Eq. (3.19) approximates G to a very high precision [better than the expression in Eq. (3.18)]. Therefore it can be used to observe the dominant effects due to rotation. It is seen from this simple expression that rotation has practically no effect on the field magnitude. It essentially affects the phase by inducing a Doppler-like local shift of the field *wavelength*. This effect is maximal along the line tangential to its motion (e.g., the line $x=x'=5\lambda$ in Fig. 1), and is vanishingly small along a line that is normal to the source motion (e.g., the line $y=0$ in Fig. 1). The latter is seen very clearly also in Fig. 4, as the difference between the stationary and rotating cases vanishes along the line $y=0$. It should be emphasized, however, that this wavelength shift is *not* the frequency shift usually seen in classical Doppler effect: in the rotating reference frame, the field oscillates at the single frequency ω, independently of the source and observation points $(\boldsymbol{r},\boldsymbol{r}')$ which move together with the medium. The effect is observed only on the field *wavelength*, and not on its frequency.

Another point worth examining is the source-free structure of the fields. From the constitutive relations in Eqs. (2.3a), (2.3b), (2.4), and (2.8), we get for the TM polarization

$$\boldsymbol{D} = \hat{z}(\epsilon E_z + c^{-2}\Omega\rho H_\rho), \tag{5.1a}$$

$$\boldsymbol{B} = \mu \boldsymbol{H}_t + c^{-2}\Omega\boldsymbol{\rho}E_z = \frac{-i}{\omega}(\boldsymbol{J}_t^M + \nabla_t \times \hat{z}E_z), \tag{5.1b}$$

and for the TE polarization

$$\boldsymbol{D} = \epsilon \boldsymbol{E}_t - c^{-2}\Omega\boldsymbol{\rho}H_z = \frac{i}{\omega}(\boldsymbol{J}_t + \nabla_t \times \hat{z}H_z), \tag{5.2a}$$

$$\boldsymbol{B} = \hat{z}(\mu H_z - c^{-2}\Omega\rho E_\rho). \tag{5.2b}$$

Substituting our Green's function fields, and noting that $\partial_z \equiv 0$ (two-dimensional problem), it is readily verified that the source free conditions $\nabla\cdot\boldsymbol{D}=0$, $\nabla\cdot\boldsymbol{B}=0$ are automatically satisfied whenever $\boldsymbol{J}$, $\boldsymbol{J}_t^M=0$ and $\boldsymbol{r}\neq\boldsymbol{r}'$. Furthermore, it is seen that under rotation the local transverse plane wave structure of the field E_z in TM (and H_z in TE), is the same as that of stationary system: direction of propagation is normal to polarization (since $\nabla\cdot\hat{z}E_z=0$ in the former, and $\nabla\cdot\hat{z}H_z=0$ in the latter). However, under rotation this property is generally not preserved for the field $\boldsymbol{H}_t$ in TM (since now $\nabla\cdot\boldsymbol{H}_t\neq 0$ - it depends on Ω) and for the field $\boldsymbol{E}_t$in TE (since $\nabla\cdot\boldsymbol{E}_t\neq 0$).

B. Numerical implementations

As discussed in the introduction section, a well-suited solution procedure for scattering of time-harmonic electromagnetic signal from a dielectric structure is the method of moments [9]. A vital tool here is the Green's function of an appropriately defined background medium, describing the field at $\boldsymbol{r}$ due to a unit point source at $\boldsymbol{r}'$. For scattering from a stationary structure, the background is most conveniently defined as a homogeneous medium, and the corresponding G is well known. For the analysis of scattering from a rotating structure as seen in the rotating medium rest frame, the background problem Green's function is the field in a rotating homogeneous medium where both the source point at $\boldsymbol{r}'$ and the observer at $\boldsymbol{r}$ rotate together with the medium. This is exactly the solution derived in this work. In the general solution scheme, G is used to expand the field in each homogeneous subdomain of the dielectric structure, and the requirement for satisfying boundary conditions is then imposed (see, for example, Refs. [9–11]). Fortunately, in 2D geometries rotation does not affect boundary conditions at the dielectric interface; this can be seen directly from Eqs. (2.2a), (2.2b), (2.3a), and (2.3b) and Eqs. (5.1a), (5.1b), (5.2a), and (5.2b) by applying to it the fact that the structure dielectric surfaces are invariant along the rotation axes $\hat{z}$. With this observation at hand, well tested legacy codes dealing traditionally with stationary scatterers can be extended to hold also for rotating scatterers (at their rest frame), simply by replacing the stationary medium Green's function G^{st} by the Green's function G derived in this work *and at no additional cost of algorithm complexity or programming*. With this approach, we have extended the method in Refs. [10,11] used successfully by us for stationary PhC problems, to apply for rotating crystals as well [17].

Finally, we note that the numerical implementation of MOM requires us to evaluate $G(\boldsymbol{r},\boldsymbol{r}')$ at a very large number of different points in $\boldsymbol{r}$ and $\boldsymbol{r}'$. If the exact G is used, each pair of values for $\boldsymbol{r}$ and $\boldsymbol{r}'$ requires a new spectral series summation of Eq. (3.12), over hundreds of cylindrical harmonics. This fact renders the use of the exact spectral representation of G completely impractical for many problems of interest. On the other hand, the computation of the stationary medium Green's function is relatively simple; it requires the evaluation of a single Hankel function and highly efficient commercial numerical libraries are available for this. Hence the importance of the high-quality approximate solution given in Eq. (3.19); it is expressed in terms of the stationary medium Green's function, multiplied by an exponential.

VI. CONCLUSIONS

We presented a general Green's function theory for a slowly rotating homogeneous two-dimensional medium. The theory is derived in the medium rest frame, and it provides a

systematic tool for a general study of the spectral properties of rotating systems. The classical results of the Sagnac effect can be obtained as special case or approximation, that pertains to a limited portion of the problem (full) spectra. The new Green's function can be used for a method of moment based numerical study of various electromagnetic aspects of rotating systems. It is especially needed in rotating optical systems that consist of intricate scattering effects, such as the photonic crystal optical gyroscope [3]. This use will be demonstrated in future studies.

[1] M. Skorobogatiy and J. D. Joannopoulos, Phys. Rev. B **61**, 5293 (2000).

[2] M. Skorobogatiy and J. D. Joannopoulos, Phys. Rev. B **61**, 15554 (2000).

[3] B. Z. Steinberg, Phys. Rev. E **71**, 056621 (2005).

[4] E. J. Post, Rev. Mod. Phys. **39**, 475 (1967).

[5] J. Scheuer and A. Yariv, Phys. Rev. Lett. **96**, 053901 (2006).

[6] E. J. Reed, M. Soljacic, and J. D. Joannopoulos, Phys. Rev. Lett. **90**, 203904 (2003).

[7] E. J. Reed, M. Soljacic, and J. D. Joannopoulos, Phys. Rev. Lett. **91**, 133901 (2003).

[8] T. Shiozawa, Proc. IEEE **61**, 1694 (1973).

[9] R. F. Harrington, *Field Computation by Moment Methods* (Krieger, Malabar, FL, 1982).

[10] Y. Leviatan and A. Boag, IEEE Trans. Antennas Propag. **35**, 1119 (1987).

[11] A. Boag, Y. Leviatan, and A. Boag, Radio Sci. **23**, 612 (1988).

[12] O. Painter, J. Vuckovic, and A. Scherer, J. Opt. Soc. Am. B **16**, 275 (1999).

[13] B. S. Song, S. Noda, and T. Asano, Science **300**, 1537 (2003).

[14] H. J. Arditty and H. C. Lefevre, Opt. Lett. **6**, 401 (1981).

[15] *Fiber-Optic Rotation Sensors*, edited by S. Ezekiel and H. J. Arditty, Springer Series In Optical Sciences (Springer-Verlag, Berlin, 1982).

[16] L. B. Felsen and N. Marcuvitz, *Radiation and Scattering of Waves* (Prentice-Hall, Englewood Cliffs, NJ, 1973).

[17] Ben Z. Steinberg, Ady Shamir, and Amir Boag, CWL6 paper, CLEO-QELS 2006 Conference, Long Beach CA, May 2006.